Sensors & Actuators: A. Physical 410 (2026) 118243

Contents lists available at ScienceDirect

Sensors and Actuators: A. Physical

journal homepage: www.journals.elsevier.com/sensors-and-actuators-a-physical

Fabrication and integration of partially-transparent ionic polymer–metal composite actuators into microphysiological systems

Alireza Tajeddin[a], Antonio Velarte[b], Romina Sattari[a], Maury Wiendels[c], Andres Hunt[d], Christine L. Mummery[c], Valeria Orlova[c], Juan Zhang[e], Vincent Portero[e], Esther Pueyo[b], Arantxa Otín[f], Massimo Mastrangeli[a,*]

[a] Department of Microelectronics, Faculty of Electrical Engineering, Mathematics and Computer Science, Delft University of Technology, Delft, 2628 CD, the Netherlands
[b] Biomedical Signal Interpretation and Computational Simulation (BSICoS) Group, I3A Institute, IIS Aragon, University of Zaragoza, Zaragoza, 50018, Spain
[c] Department of Anatomy and Embryology, Leiden University Medical Center, Leiden, 2333 ZC, the Netherlands
[d] MNE, Department of Precision Microsystems Engineering, Faculty of Mechanical Engineering, Delft, 2628 CD, the Netherlands
[e] Laboratory of Experimental Cardiology, Department of Cardiology, Leiden University Medical Center, Leiden, 2333 ZD, the Netherlands
[f] Group of Power Electronics and Microelectronics (GEPM) Group, I3A Institute, University of Zaragoza, Zaragoza, 50018, Spain

HIGHLIGHTS

- Developed a novel fabrication approach to achieve partially-transparent IPMC actuators with patterned electrodes.
- Enabled direct optical and fluorescence imaging through transparent windows on the actuator.
- Achieved low-voltage electromechanical stimulation within biologically-relevant regimes.
- Integrated the actuator platform into standard well plates for organ-on-chip applications.

ARTICLE INFO

Keywords:
Electroactive polymers
Fluorescence microscopy
Ionic polymer–metal composite (IPMC)
Mechanical stimulation
Microphysiological systems
Transparent actuator

ABSTRACT

We present partially-transparent ionic polymer–metal composite (IPMC) actuators and their seamless integration into microphysiological systems, to enable dynamic mechanical stimulation of cell monolayers with direct optical access. The proposed IPMC platform employs a layered microfabrication strategy that allows precise tailoring of electrode geometry while preserving optical transparency across selected regions of the actuator. This design overcomes a key limitation of conventional IPMCs, namely their inherent opacity and resulting lack of (bio-)opto-mechatronics compatibility, thereby facilitating *in vitro* applications and real-time optical and fluorescent microscopy. The actuators are integrated into standard 12-well culture plates through customized mechanical and electrical interfaces and are driven by a compact, programmable electronic control system, enabling flexible modulation of actuation dynamics within biologically-relevant regimes. We confirm the biocompatibility of the platform by culturing Human Embryonic Kidney (HEK) cells and contractile cardiomyocytes from human-induced pluripotent stem cells (hiPSC-CMs). Together, these advances establish a scalable, low-voltage, and optically-compatible actuation platform for organ-on-chip and mechanobiology applications.

1. Introduction

Despite the widespread reliance on pharmaceuticals to manage human health conditions, concerns persist regarding their safety, efficacy, and translational success. While drug-based therapies have substantially improved life expectancy and therapeutic outcomes, up to 90% of drug candidates still fail during clinical trials, largely due to the limited predictive power of preclinical models [49]. Conventional animal-based preclinical models remain ethically contentious but, as importantly, frequently fail to capture human-specific physiological responses because of fundamental interspecies differences in metabolism, tissue architecture, and cellular signaling pathways [47]. These limitations underscore an urgent need for human-relevant experimental platforms that more accurately recapitulate *in vivo* physiology.

* Corresponding author.
Email address: m.mastrangeli@tudelft.nl (M. Mastrangeli).

https://doi.org/10.1016/j.sna.2026.118243
Received 31 March 2026; Received in revised form 2 July 2026; Accepted 14 July 2026
Available online 17 July 2026
0924-4247/© 2026 The Author(s). Published by Elsevier B.V. This is an open access article under the CC BY license (http://creativecommons.org/licenses/by/4.0/).

Organ-on-chip (OoC) technologies are emerging as a promising class of microphysiological systems (MPS) designed to address this need. By combining microfabrication, microfluidics, and cell biology, OoC platforms enable the controlled reconstruction of tissue-level organization and function within well-defined microenvironments [33]. When integrated with human stem-cell–derived tissues in particular and micro-engineered features, OoCs offer scalable and patient-specific models for disease investigation, drug screening, and personalized medicine [35]. However, despite these advances, OoC systems may still only partially or selectively reproduce the full functional complexity of native organs.

A key limitation lies in the insufficient representation of dynamic mechanical cues. *In vivo*, cells are continuously exposed to biomechanical stimuli such as shear stress, compression, and cyclic tensile strain, which critically regulate cellular morphology, maturation, and function through mechanotransduction pathways [9,18]. Numerous studies have demonstrated that the absence of such cues in static culture systems leads to altered gene expression, impaired tissue functionality, and non-physiological drug responses [8]. Consequently, recent MPS research increasingly emphasizes not only biochemical and architectural fidelity, but also the precise reproduction of dynamic mechanochemical environments [53,54].

Among mechanical stimuli, tensile stress plays a particularly prominent role in musculoskeletal and cardiovascular tissues. Longitudinal strain strongly influences myofibrillar alignment, sarcomere organization, and force generation in striated muscle, including cardiac and skeletal muscle constructs [13]. Accordingly, OoC platforms modeling mechanically-active tissues increasingly incorporate substrate stretching or dynamic loading mechanisms to better emulate native biomechanical niches.

To date, tensile stimulation in MPS has been primarily achieved using motor-driven stretchers or pneumatically-actuated elastic membranes. Motorized systems offer precise control over strain amplitude and frequency and have been widely used to study mechanotransduction in stem cell derivatives, endothelial cells, and muscle tissues [15,21,27,30,41]. However, their reliance on bulky external hardware, their limited scalability, and restricted integration with microfluidic platforms constrain their applicability in compact OoC systems. Pneumatic approaches, including lung- and muscle-on-chip devices, enable on-chip deformation and improved compatibility with microfluidics, but often require complex multilayer fabrication, tight vacuum control, and careful strain calibration [10,17,26,34,48]. Collectively, these limitations motivate alternative actuation strategies that are compact, electrically-driven, and readily-integrable.

Electroactive polymers (EAPs) provide a compelling route toward on-chip mechanical actuation. These materials convert electrical stimuli directly into mechanical deformation, enabling simple actuator constructions that are miniaturizable, compliant, lightweight, and biocompatible without external pumps or motors [1,6,23]. Ionic EAPs are particularly suitable for aqueous and biological environments, as they operate at low voltages on the principle of physical transportation of ionic species in an electric field. They include ionic polymer–metal composites (IPMCs), conducting polymers, and ionic gels [32,38]. In contrast, electronic EAPs such as dielectric elastomers offer large strain and fast response but require high driving voltages, which can complicate biological integration [4,12,40].

Among ionic EAPs, IPMCs are especially attractive for OoC applications. These actuators consist of an ion-exchange polymer membrane, such as Nafion™, sandwiched between conductive electrodes. Nafion™ is a perfluorosulfonic acid ionomer consisting of a semi-crystalline polytetrafluoroethylene (PTFE) backbone with sulfonic acid-terminated side chains. The contrast between the hydrophobic fluorocarbon backbone and the hydrophilic ionic side chains leads to phase separation, which becomes more pronounced upon hydration. As a result, interconnected ionic domains and channels are formed within the polymer matrix, enabling efficient ion and solvent transport [14,28]. The morphology and transport behavior of Nafion™ are strongly influenced by hydration level,

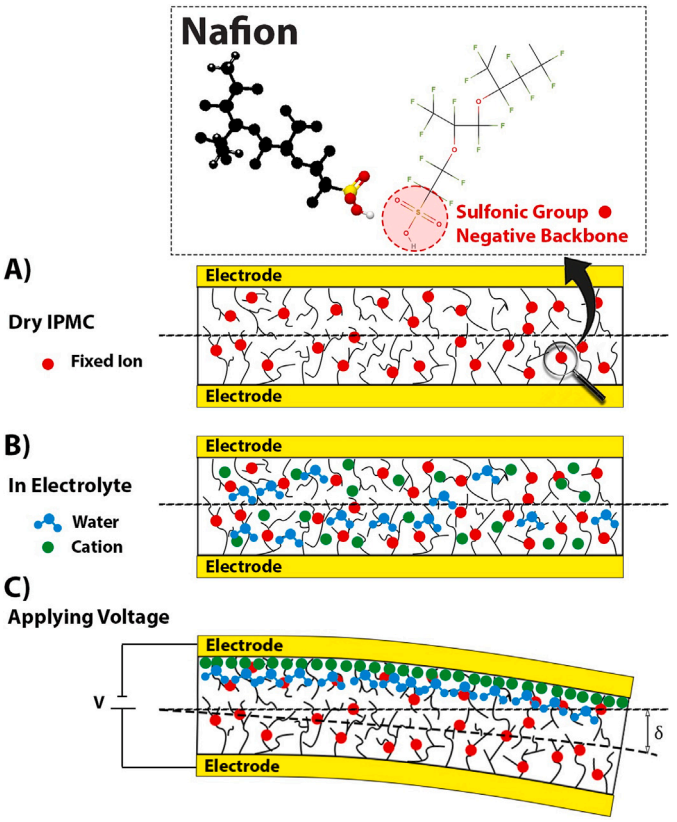


Fig. 1. A) Structure of a dry IPMC actuator. Inset: Morphology of Nafion illustrating phase separation into a hydrophobic polymer backbone and hydrophilic ionic channels. B) IPMC actuator in a water-based electrolyte (e.g., cell medium). C) Actuation mechanism of the IPMC under electric voltage driving.

solvent history, and environmental conditions, which in turn affect its electrochemical and mechanical properties [22,43]. These characteristics make Nafion™ one of the most widely used ionic polymers for ionic polymer–metal composites (IPMCs), where electrically-induced ion migration and solvent redistribution generate macroscopic deformation under low driving voltages. Furthermore, the nano-phase-separated structure plays a critical role in determining the coupling between ionic transport and mechanical actuation, making an understanding of its morphology important for the design and optimization of IPMC-based devices [20,43]. Ion migration upon low-voltage stimulation of an IPMC (typically within ±5 V) redistributes ions and solvent across the membrane thickness (Fig. 1), generating a non-uniform stress field that causes the IPMC to bend [44]. IPMCs combine low-voltage operation, mechanical compliance, operation in hydrated environments, and compatibility with miniaturization and shaping. Recent reviews have highlighted substantial advances in IPMC materials, electrode engineering, and actuation performance, while also identifying challenges related to fabrication scalability, long-term stability, and optical transparency [3,29,52].

The lack of optical transparency, primarily arising from opaque electroless-plated metal electrodes, remains a critical barrier to integrating IPMCs into OoC platforms that rely on real-time optical monitoring and fluorescence microscopy [36,37]. Several approaches have been proposed to address this limitation. Jeon et al. used tape-based patterning compatible with electroless plating, enabling additional degrees of freedom in the actuator and allowing fish-like locomotion [19]. Similarly, Shin et al. patterned electrolessly-plated IPMC electrodes using a commercial milling machine [46]. In this work, we address this limitation by introducing a fabrication strategy based on e-beam evaporated thin metallic electrodes, which enables semi-transparent IPMC actuators

compatible with live-cell imaging and scalable microfabrication. Beyond material and fabrication advances, the present platform targets operation within the microstrain regime, rather than aiming for large tissue-scale deformations. This enables the controlled delivery of relatively small cyclic strains that are increasingly recognized as biologically meaningful, particularly in emerging studies of nuclear mechanotransduction, mechanosensitive ion-channel regulation, and mechanically-driven cell-state transitions [51]. By accessing this ultra-sensitive strain regime, the proposed approach establishes a scalable and modular foundation for future strain-amplification strategies, while preserving compatibility with optical microscopy and integrated OoC systems.

2. Concept and design rationale

As described in detail in the previous section, ionic polymer–metal composites (IPMCs) typically consist of an ion-conductive polymer (ionomer) backbone (e.g., Nafion™), sandwiched between two noble metal electrodes (e.g., Pt or Au), mainly to prevent undesired (electro)chemical reactions. Nafion™, the most widely-used ionomer for IPMC fabrication, is composed of a fluoropolymer backbone (similar to Teflon) and sulfonic acid side groups, that are terminated by protons and can be exchanged for various other cations (Fig. 1).

For bioapplications such as *in vitro* cell cultures, the material must meet several criteria, among which biocompatibility and optical transparency are the most critical. In bio-integrated actuation systems, optical transparency is essential for real-time observation of cellular responses, while mechanical actuation enables dynamic stimulation of cells. However, achieving both high optical transmittance and suitable electromechanical performance presents a key design trade-off in IPMCs.

In an IPMC cantilever structure, the metal electrodes on each side of the Nafion™ membrane, which is itself optically transparent, make the cantilever opaque. To achieve optical clarity while maintaining performance, the IPMC design proposed in this work introduces transparent windows through electrode patterning. The electrode geometry can be shaped to locally enhance optical transmission without globally compromising charge transport or actuation strains. Identical axio-symmetric patterns were implemented on both sides of the membrane to achieve transparency and produce uniform bending deformation (Fig. 2).

Since Nafion™ is inherently transparent [39], the resulting cantilever exhibits partial transparency, enabling concurrent optical access through the window and mechanical actuation. This configuration allows the IPMC to function as a dynamic, biocompatible substrate suitable for cell culture and mechanical stimulation studies, particularly in bioelectronic and OoC platforms.

3. Materials & methods

Nafion™ was selected as the ionic polymer substrate due to its high ionic conductivity, chemical stability, optical transparency, and

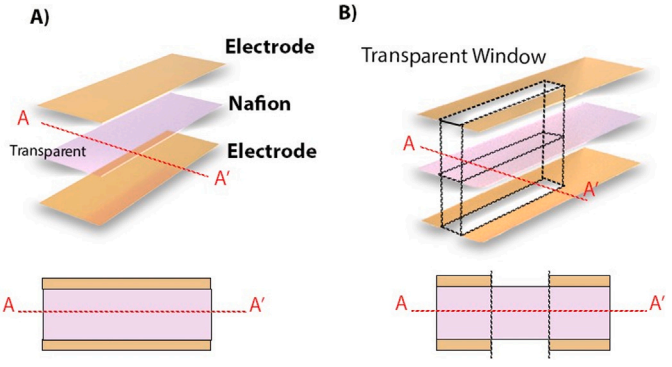


Fig. 2. Structure (top) and cross-sectional view (bottom) of A) standard IPMC cantilever with opaque metallic electrodes and of B) the proposed IPMC with a transparent window patterned into its electrodes.

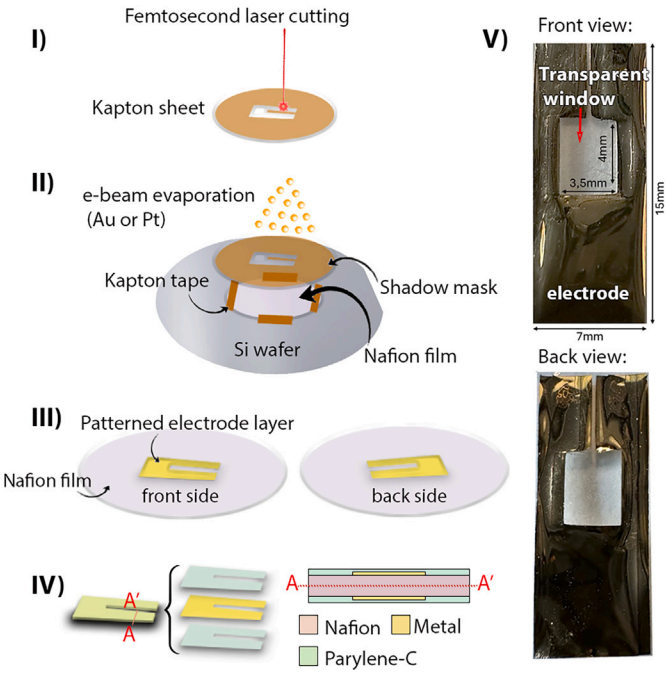


Fig. 3. Fabrication process of semi-transparent IPMC actuators: (i) shadow mask patterning by laser cutting a 50 μm-thick Kapton sheet; (ii) placement of the Nafion™ film on a Si wafer, and metal deposition through the shadow mask; (iii) electrode patterning is repeated on both sides of the Nafion™ substrate; (iv) encapsulation of the actuator with Parylene-C; (v) fully-processed partially-transparent IPMC actuator.

widespread use in IPMC actuators. The electromechanical response of Nafion-based IPMCs originates from the migration of hydrated ions within the polymer under an applied electric field. Therefore, preserving the integrity of the ionic transport network during fabrication is critical for actuator performance. Unlike many polymeric materials, oxygen plasma treatment is generally not suitable for Nafion™, as plasma exposure can damage the sulfonic acid side chains and disrupt the ionic domains responsible for ion transport. This degradation may reduce water uptake and ionic conductivity, ultimately compromising actuator performance [2]. For this reason, oxygen plasma treatment was avoided during device fabrication. Furthermore, conventional microfabrication and patterning techniques are often incompatible with Nafion™ films. For instance, spin-coating photoresist directly onto Nafion™ typically causes substrate swelling, making standard lithographic processes impractical. Similarly, the use of adhesive interlayers commonly employed for noble metals, such as Au or Pt, proves unsuitable for Nafion™. These adhesion-promoting layers (e.g Cr or Ti) tend to diffuse into the polymer bulk and interact with the negatively-charged sulfonate groups of the backbone, leading to partial blockage of ionic sites and a consequent reduction in actuation performance [16].

To overcome these challenges, we exploited the porous nature of Nafion™ and employed high-vacuum e-beam evaporation with shadow masking to achieve patterned metal deposition with enhanced metal adhesion and penetration into the polymer surface (Fig. 3). IPMC actuators were fabricated using 50 μm-thick Nafion™ 212 (Ion Power, USA) fixed on a 4-inch silicon wafer with Kapton tape. Electrodes were sequentially deposited via e-beam evaporation on both sides through a 50 μm-thick laser-cut Kapton shadow mask (Lasea femtosecond laser cutter, 515 nm, 1.5 W, 250 mm s^{-1}, 22 repetitions). Before the second metal deposition, the shadow mask was aligned manually with the prior deposition to enforce the patterning of a fully-transparent optical window through the IPMC with a precision of 146.0 ± 34.2 μm (mean ± SD, n = 4). Au and Pt films with thicknesses of 100 nm and 200 nm

respectively, were deposited by e-beam evaporation under low-pressure and low-temperature conditions (2×10^{-1} mTorr, 70 °C, and a deposition rate of 3 $Å s^{-1}$). Finally, the IPMC cantilever was encapsulated by a 1.4 μm-thick layer of Parylene-C deposited from vapor phase (SCS™ coating machine, using 3 g Parylene-C dimer, GALAXYL®). An example of a semi-transparent IPMC cantilever is shown in Fig. 3(V).

3.1. Characterization methods

To characterize the samples, several complementary analyses were performed, including cross-sectional material characterization, electrical evaluation of the electrodes, and measurements of actuation performance.

3.1.1. Material characterization

Material characterization was performed using scanning electron microscopy (SEM) and energy-dispersive X-ray spectroscopy (EDX) to examine the electrode morphology and interfacial structure. Cross-sectional SEM imaging was used to determine the penetration depth of the deposited metallic layer and to identify any potential diffusion of electrode material into the Nafion™ bulk. Surface imaging was also carried out to assess the uniformity and continuity of the electrode film under the selected deposition conditions. Complementary EDX analysis provided elemental mapping to confirm the presence and distribution of metallic species within the polymer matrix. This combination of SEM and EDX offers a comprehensive understanding of both the surface and subsurface characteristics of metal–polymer interfaces, which is crucial for evaluating electrode integrity and potential contamination effects [45].

3.1.2. Electrical characterization

The electrical characterization of the samples was conducted using a two-probe measurement setup to evaluate the surface conductivity and continuity of the deposited electrode films. Given the small thickness of the metallic layers and their deposition on a soft polymer substrate, the two-probe method was selected as a straightforward and reliable approach to verify electrical connectivity across the electrode surface. Measurements were performed using a precision probe station (Cascade Microtech, Inc.) under ambient conditions, ensuring minimal contact resistance by applying uniform probe pressure. This characterization allowed confirmation of the electrode integrity and assessment of possible discontinuities or high-resistance regions arising from surface defects or microcracks. Furthermore, the sheet resistance was also measured using a soft-tipped probe station (Ossila) to ensure that the thin film was characterized without damage.

3.1.3. Mechanical characterization

Dynamic mechanical analysis (DMA) was carried out using a TA Instruments Q800 system to evaluate the mechanical properties of the samples. The measurements were performed to compare the viscoelastic behavior of Nafion™ with and without metallic electrodes, allowing assessment of the effect of electrode deposition on the polymer's stiffness and damping characteristics. Rectangular specimens were tested in tension mode under controlled temperature to ensure reliable comparison. DMA provides sensitive insight into changes in the storage and loss moduli, which reflect both the mechanical reinforcement and potential constraint effects introduced by the electrode layers [31,42].

3.1.4. Optical transmission

Optical transparency of the samples was evaluated using UV–visible (UV–vis) spectroscopy (Perkin Elmer 1050 UVVISNIR Spectrophotometer) by measuring their transmission over the 250–800 nm wavelength range. Samples were mounted in the spectrophotometer beam path, and a matching uncoated glass substrate was used as the reference to eliminate background absorption and reflection effects. Transmission spectra were recorded with a 10 nm step size and normalized to the reference signal. The average transmittance in the visible region (400–700 nm) was used to assess overall transparency, while the ultraviolet region (200–400 nm) was examined to detect absorption at shorter wavelengths relevant to fluorescence microscopy. Particular attention was given to the 350–500 nm range, where common fluorophores are excited; high transmission and the absence of significant absorption bands in this region confirm suitability for fluorescence imaging.

3.1.5. Actuation characterization

The actuation behavior of the samples was evaluated using a custom-built setup designed to control the input voltage and record the resulting mechanical and electrical responses. A sinusoidal voltage signal with fixed amplitude was applied while sweeping the excitation frequency logarithmically from 0.1 to 30 Hz in 20 discrete steps, using a PC computer with NI LabVIEW 2018 software, an NI USB-6211 data acquisition card and an LM675T-based custom amplifier. The tip displacement of the actuator was measured in PBS (Phosphate-Buffered Saline), which primarily contains sodium (Na^+) and potassium (K^+) cations, in real time using a Micro-Epsilon laser displacement sensor (OptoNCDT 1900-10), providing high-resolution tracking of the dynamic response, with the same NI USB-6211 and LabVIEW 2018 software. Simultaneously, the impedance of the IPMC was monitored throughout the actuation cycle to correlate the electrical characteristics with the mechanical output. This integrated approach allowed assessment of frequency-dependent performance and provided insight into the electro-mechanical coupling behavior of the actuator under controlled excitation conditions.

Under voltage-induced bending, the surface strain of the IPMC cantilever was quantified using a geometric bending model that relates the measured tip displacement to the curvature of the beam. Assuming the deformed cantilever approximates an arc of a circle, the radius of curvature R is obtained from the tip deflection δ (see Fig. 1(C)) and the free length L (see Fig. S1 in Supplementary Data).

The axial strain at the outer surface is then expressed as $\varepsilon = d/R$, where d is the thickness of the actuator. Combining these relations yields the strain expression:

$$\epsilon(\%) = \frac{2d\,\delta}{L^2 + \delta^2} \times 100 \tag{1}$$

This curvature-based method follows directly from classical Euler–Bernoulli beam theory and has been employed extensively for experimental IPMC characterization [24].

3.1.6. Experimental setup

A custom-built experimental setup was developed to drive the actuation of the IPMC samples under cell culture conditions. The electronics combine a microcontroller unit that generates arbitrary low-frequency waveforms with digitally-programmable amplitude regulation and two independent analog output channels (which can operate either synchronously or independently) capable of 20 V and 500 mA of voltage and current output, respectively. A printed circuit board (PCB) shield ensures a compact footprint and plugs directly into an STM32 NUCLEO board, while a Python-based graphical interface provides intuitive configuration and seamless laboratory integration. The actuator clamps were specifically designed to fit within a standard 12-well plate, enabling direct integration with biological assays (Fig. 4(A)). These clamps were fabricated using high-resolution 3D printing to ensure accurate alignment, mechanical stability, and chemical compatibility with the culture environment. The actuator is connected to Au-plated clamps interfaced with a PCB that supplies the driving voltage (Fig. 4(B)). This setup provides a compact and reproducible platform for studying the electro-mechanical stimulation of cells through IPMC-based actuators (Fig. 4C).

3.1.7. Biocompatibility and fluorescence imaging compatibility

The biocompatibility of the partially-transparent IPMCs was evaluated using direct cell culture, proliferation, and viability assays.

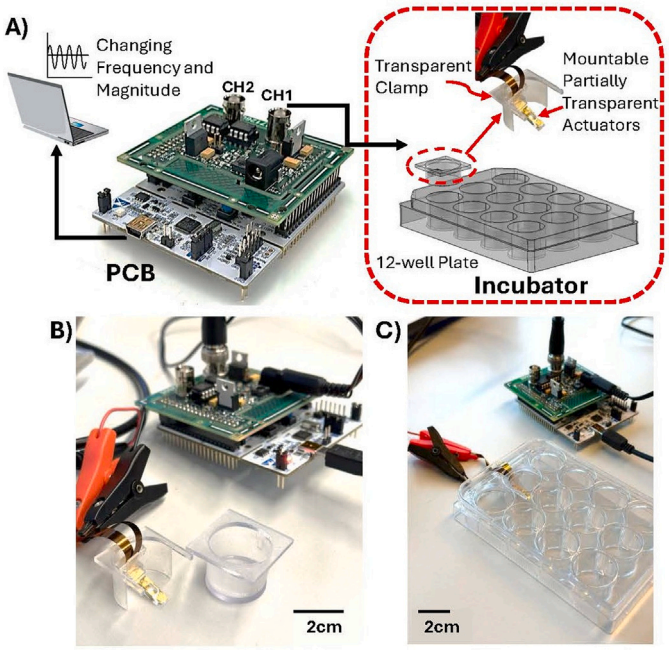


Fig. 4. A) Schematic of the experimental setup. B) Transparent clamp fabricated by 3D-printing. C) Experimental setup fitting a standard 12-well plate.

In addition, a separate experiment was conducted to assess the compatibility of the IPMCs with fluorescence imaging through the membrane.

Direct cell culture assay

Human-induced pluripotent stem cell-derived cardiomyocytes (hiPSC-CMs), which are contractile cells, were used for this assay. Prior to cell seeding, the substrates were activated and sterilized by plasma treatment to improve surface wettability and prevent contamination. To assess cytocompatibility, activated membranes were coated with Matrigel and seeded with hiPSC-CMs differentiated and cultured from the hiPSC line LUMC99, as described previously [5]. hiPSC-CMs were maintained in mBEL medium supplemented with ITS-X and Lipids, which was selected as it provides a consistent culture environment routinely used for both hiPSC differentiation and long-term cardiomyocyte maintenance, requiring only modifications in the supplementation of small molecules to transition between differentiation and maintenance stages. Cells were cultured under standard incubation conditions (37 °C, 5% CO_2, humidified atmosphere). Cell morphology, attachment, and viability were monitored for up to 10 days.

Proliferation assay

Human embryonic retinal PER.C6 cells were dissociated using TrypLE Express Enzyme (Thermo Fisher Scientific) and seeded on gelatin-coated Nafion membranes and in standard 12-well cell culture plates. Cells were cultured in Dulbecco's Modified Eagle Medium (DMEM, Life Technologies) supplemented with 10% fetal bovine serum (FBS, Serana), 10 mM $MgCl_2$, and penicillin/streptomycin (Life Technologies). Cell cultures were imaged daily from the day of seeding (Day 0) using an EVOS™ M3000 Imaging System (Thermo Fisher Scientific) equipped with bottom illumination and top image acquisition.

Viability assay

Cell viability was assessed using a Trypan Blue exclusion assay. After PER.C6 cells reached confluency under both culture conditions (3 days post seeding), cells were dissociated and pelleted by centrifugation (10 min, room temperature, 140 × g). The resulting pellet was resuspended in culture medium, and 10 µL of the cell suspension was mixed with 10 µL of Trypan Blue Dye solution (Bio-Rad). Subsequently, 10 µL of the stained cell suspension was loaded into a cell counting chamber (Corning BV), and live and dead cells were quantified using a Cytosmart automatic cell counter (Corning). Viability measurements were performed on five independent membrane cultures and four independent well plate cultures, resulting in a total of 36 viability measurements.

Fluorescence imaging assay

Human Embryonic Kidney cells (HEK293T) were used to examine the compatibility of our partially-transparent actuating substrate with optical and fluorescence imaging. HEK293T cells were seeded onto the device membrane after coating with 1% bovine gelatin (Sigma). Cells were cultured in DMEM high-glucose medium supplemented with 10% FBS and penicillin/streptomycin (Life Technologies) under standard incubation conditions (37 °C, 5% CO_2, humidified atmosphere). After 24 h, cells were co-transfected using Polyethylenimine MAX (Polysciences Europe) with two plasmids: one expressing GFP and the other mCherry under the human ubiquitin C promoter. Live-cell fluorescence imaging was performed 24 h post-transfection using an EVOS™ M3000 Imaging System (Thermo Fisher) with bottom illumination and top acquisition. For fixed-cell imaging, the cells cultured on the membranes were fixed in 4% formaldehyde for 30 min at 4 °C, washed with PBS, permeabilized with 1% Triton X-100 in PBS for 10 min, and stained with Hoechst for nuclear labeling. Samples were washed with PBS and mounted on coverslips using VECTASHIELD mounting medium (Vector Laboratories, H-1000). Mounted samples were stored in the dark at room temperature for 24 h to allow polymerization before imaging with a Nikon Eclipse 80i fluorescence microscope (Nikon Instruments). Importantly, in this configuration, the excitation fluorescence light first passed through the transparent Nafion membrane, excited the respective fluorochrome which then emitted a fluorescent signal recorded from the top.

4. Results and discussion

To achieve a scalable and partially-transparent IPMC actuator, electron-beam (e-beam) evaporation was employed as an alternative to conventional electroless plating methods. The common practice of introducing an adhesive interlayer to improve noble metal adhesion proved unsuitable for Nafion™, as these layers (e.g., Cr or Ti) readily oxidize and diffuse into the polymer bulk, interacting with the negatively-charged sulfonate groups and thereby suppressing ionic transport, as illustrated in Fig. 5(A) and (B). Additionally, plasma treatment of Nafion™ was found to further deteriorate the actuator's performance, consistent with previous reports showing that plasma exposure can reduce both ion conductivity and surface hydrophilicity [2]. Consequently, the most effective approach for achieving uniform and conductive thin-film electrodes was to exploit the inherent porous morphology of Nafion™, which facilitates metal infiltration and adhesion without chemical modification. This strategy represents a novel direction in thin-film deposition on porous ionic polymers. Two noble metals, gold (Au) and platinum (Pt), were investigated as electrode materials, both individually and in sequential combination; co-deposition of these inert metals on Nafion™ remains a challenging but promising route for optimizing conductivity and durability.

By leveraging the intrinsic porosity of Nafion™, both metals were successfully integrated without the use of intermediate adhesive layers. In this configuration, Pt primarily contributes to enhancing the structural rigidity and durability of the cantilever, while Au exhibits superior penetration into the polymer matrix, promoting more efficient charge transfer across the electrode–electrolyte interface. Cross-sectional EDX analysis confirmed the presence and depth distribution of both metals within the Nafion™ bulk, verifying their complementary roles in achieving a uniform and mechanically robust electrode structure (Fig. 5(C)).

The deposited electrodes exhibited sufficient adhesion to withstand mechanical abrasion, as confirmed by a standard scratching test. However, delamination occurred when the samples were immersed in aqueous environments such as water or phosphate-buffered saline

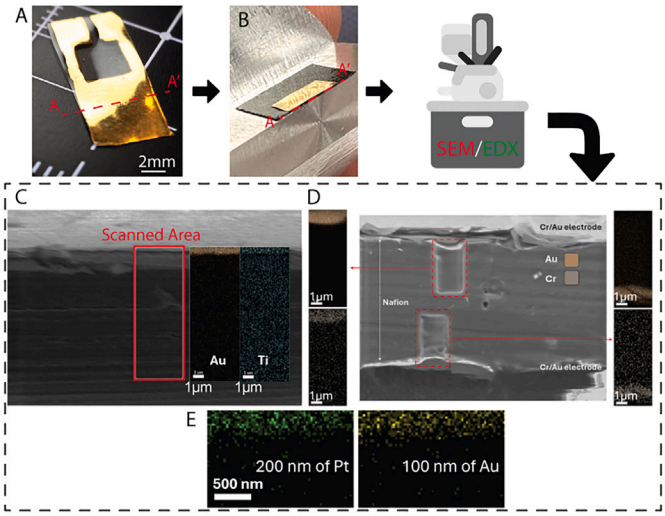


Fig. 5. (A) Au-coated sample incorporating a Ti/Cr adhesion layer. (B) Preparation of the sample cross-section for SEM and EDX characterization. (C) Diffusion of Ti and contamination of the bulk of Nafion™ by Ti. (D) Diffusion and contamination of Nafion™ bulk by Cr (red dashed boxes indicate the scanned areas in the sample cross-section, Nafion thickness is 50 μm). (E) Comparing the diffusion depth of 100 nm of Au to 200 nm of Pt in the Nafion™ matrix during high-vacuum e-beam evaporation. (For Interpretation of the references to colour in this figure legend, the reader is referred to the web version of this article.)

(PBS), primarily due to solvent diffusion and the resulting swelling of the Nafion™ matrix. To address this limitation, several encapsulation strategies were explored. Although polydimethylsiloxane (PDMS) was initially considered, its use proved impractical because the Nafion™ substrate swelled upon contact with the uncured PDMS mixture, compromising the uniformity. In contrast, chemical vapor deposition (CVD) of Parylene-C at room temperature was identified as the most effective encapsulation approach, providing a conformal, pinhole-free barrier that preserved electrode integrity while maintaining the flexibility and functionality of the actuator.

The electrical properties of the deposited electrodes were evaluated using a two-probe I–V measurement. The curve obtained (Fig. 6(A)) exhibits a straight line through the origin, indicating ohmic behavior and confirming good electrical contact across the film. This linearity suggests that the thin metallic layer forms a continuous and uniform conductive path on the Nafion™ surface without significant interfacial barriers or discontinuities. The sheet resistance of the Au and Au/Pt layer was measured as ~ 359.32 Ω and ~ 15.40 Ω respectively.

Dynamic mechanical analysis (DMA) was performed to evaluate the influence of the metallic electrode layers and encapsulation on the mechanical behavior of the Nafion™ substrate. As shown in Fig. 6(B), the stress–strain response of the Pt- and Au-coated samples, encapsulated with a 1.4 μm-thick layer of Parylene-C, follows a similar trend to that of pure Nafion™, indicating that the intrinsic viscoelastic behavior of the polymer is largely retained. The slope of the initial linear elastic region was used to estimate the effective Young's modulus of each sample. The coated and encapsulated samples exhibit slightly higher stiffness (respectively 257 MPa and 280 MPa for Au electrode and Au/Pt electrodes, compared to 246 MPa for uncoated Nafion; see Fig. S2 in the Supplementary Data) due to the reinforcing effect of the metallic and polymeric surface layers, which restrict molecular mobility near the interface. However, beyond approximately 30% strain, the slope of the pure Nafion™ curve becomes higher than that of the metal-coated samples, suggesting that the encapsulation and electrode layers limit extensibility by constraining polymer relaxation.This also can be confirmed by comparing to Au-coated sample without Pt. The reduced stress response in the plastic region for both coated samples, compared to Nafion™, suggests an effect of the fabrication process, particularly the deposition temperature (70 °C), which may relax the polymer network and alter the Nafion microstructure. The higher stress observed in the Au/Pt sample indicates that the Pt layer provides additional mechanical reinforcement to the electrode stack. Overall, the results confirm that the deposition and encapsulation processes only modestly increase structural rigidity without compromising the inherent flexibility required for actuation.

The actuation performance of the samples was evaluated by applying a sinusoidal input voltage while sweeping the excitation frequency from 0.1 to 30 Hz. The resulting displacement amplitude, normalized by the input voltage (mm/V), was plotted as a Bode diagram, as shown in Fig. 6(C). Both the Pt-based and Au/Pt-coated actuators exhibited the characteristic response of a second-order electro-mechanical system, with displacement decreasing gradually at higher frequencies. In the low-frequency range (1-2 Hz), which is most relevant for soft actuation and bio-inspired applications, the Au/Pt-coated actuator demonstrated a marked improvement in performance, exceeding the displacement of the Pt-only sample by more than 100% at these frequencies. This enhancement can be attributed to the synergistic effect of the two metals: Au improves charge transfer via enhanced ionic interaction with the polymer and, due to its ductility, can accommodate deformation under cyclic strain. Pt, being harder and more brittle, contributes mechanical stability and uniform charge distribution. The combination of Au and Pt domains may allow relative movement during deformation, thereby preserving or enhancing conductivity under repeated loading. Although the resonance peak at higher frequencies appeared slightly damped in the Au/Pt sample, likely due to increased stiffness and mass, the overall response appeared more stable and controllable. These findings suggest that combining Au and Pt yields a balanced improvement in both actuation amplitude and dynamic stability, providing an effective strategy for optimizing IPMC performance in low-frequency regimes. For benchmarking purposes, the frequency response of the e-beam–evaporated actuators was compared with that of a reference sample fabricated using conventional electroless plating [37] (Fig. 6(C)). The comparison, based on displacement amplitude per unit input voltage, considered differences in electrode thickness, surface area, and fabrication complexity. Despite the significantly thinner electrodes produced by e-beam evaporation and the simpler, more controllable process, both approaches achieved comparable actuation performance, delivering maximum tip displacements on the order of 200 μm corresponding to a strain of 0.01%. This result highlights the effectiveness of the e-beam deposition method in producing high-quality, thin, and uniform electrodes capable of matching the performance of thicker, chemically-deposited counterparts, while offering superior scalability and patterning precision for microscale applications. Functional actuation after 15 days of immersion in PBS was also demonstrated (see Fig. S3 in Supplementary Data)

UV–Vis spectroscopy showed that the membrane exhibits high optical transparency in the visible range, with a transmittance of at least 90% between 400–700 nm (Fig. 7(A)). This indicates that the material is well-suited for applications requiring optical access, such as microscopy and cell imaging. Additionally, the measured absorbance within the wavelength range commonly used for biological staining is low (less than 0.05), suggesting that the membrane does not significantly interfere with typical optical staining techniques (Fig. 7(B)). These results confirm that the material maintains excellent transparency while remaining compatible with standard bioimaging methods.

Biocompatibility was first assessed using hiPSC-CMs as a direct cell culture assay. Cells readily attached, spread, and remained viable on the membrane surface, exhibiting normal morphology over a culture period of up to 10 days (Fig. 8(A)–(B)). No noticeable differences in cell attachment or morphology were observed compared with standard culture substrates, suggesting that the electrode materials, encapsulation layer, and fabrication residues did not induce detectable cytotoxic effects.

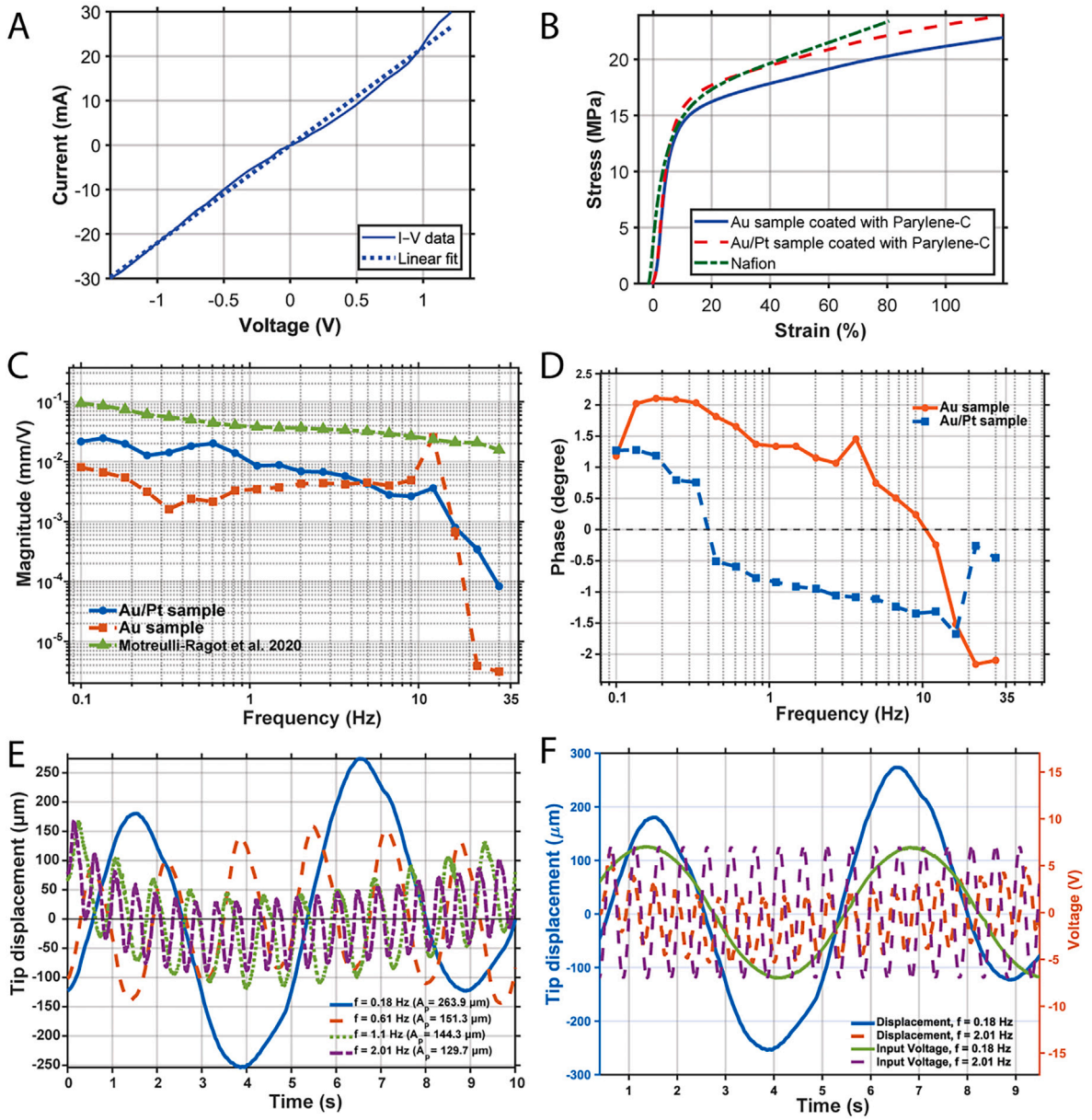


Fig. 6. (A) Electrical characterization of the deposited Au layer. (B) Comparing stress-strain results of pure Nafion™ versus the sample with metal and Parylene-C. (C) Frequency response (Bode diagram) of different samples compared to literature values. (D) Phase response of the Au and Au/Pt IPMC actuators as a function of excitation frequency, showing the frequency-dependent phase lag between the applied voltage and mechanical displacement. (E) Tip displacement of the Au/Pt sample vs time for different frequencies and a fixed voltage (10 V). (F) Comparison of the input voltage and actuation response of the Au/Pt sample at two different frequencies.

To evaluate the compatibility of the partially-transparent IPMC actuators with fluorescence microscopy, HEK293T cells were cultured and transfected directly on the actuator surface. Successful co-transfection was achieved 24 h after seeding, and the expression of GFP and mCherry in live cells was confirmed by fluorescence microscopy (Fig. 8(C)–(D)). Importantly, the transfection procedure did not alter the membrane structure, confirming compatibility with standard genetic modification protocols.

Fluorescence imaging of fixed samples showed clear positive signals in all channels, including GFP (488 nm excitation, FITC/GFP filter), mCherry (561/587 nm excitation, TRITC/mCherry filter), and Hoechst nuclear staining (350–405 nm excitation, DAPI filter) (Fig. 8(E)–(F)). These results demonstrate that the optical transparency of the membrane enables live-cell fluorescence microscopy and conventional fixed-cell immunostaining while preserving cell attachment and membrane integrity. The membrane transparency further supports optical approaches such as optogenetics, live-cell imaging, and dye-based readouts during device actuation.

Together, the results obtained with hiPSC-CMs and HEK293T cells provide qualitative evidence of cytocompatibility and demonstrate the compatibility of the developed partially-transparent IPMC platform with fluorescence-based imaging techniques, supporting its potential integration into bio-interactive systems and microphysiological platforms.

To further assess the cytocompatibility of the actuator substrate, PER.C6 cells were cultured directly on the actuator and compared with cells cultured in conventional 12-well plates. Representative images of PER.C6 cell proliferation on the actuator substrate and standard tissue culture substrates are shown in Fig. 9(A–C) and in Fig. S4 of

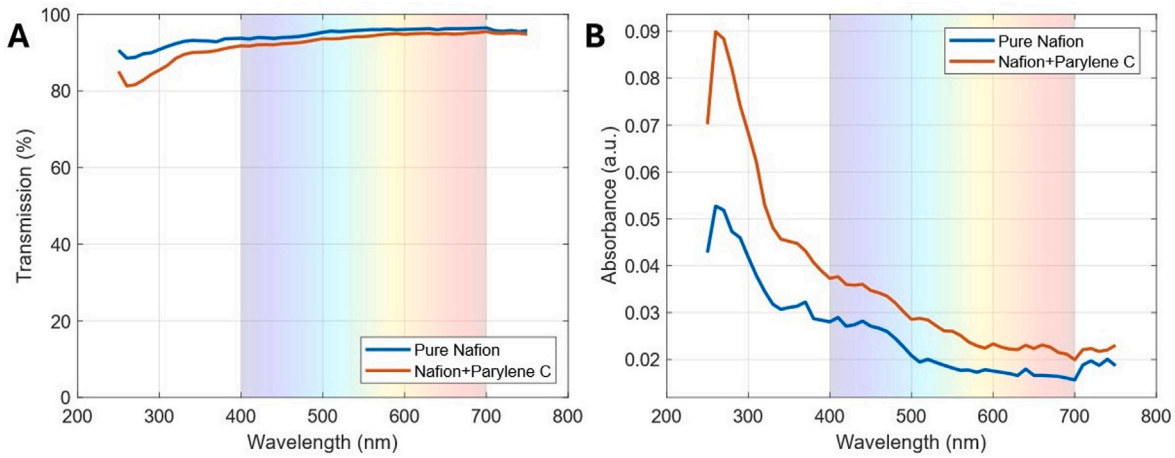


Fig. 7. Comparing the optical transparency of pure Nafion with Parylene-coated Nafion.

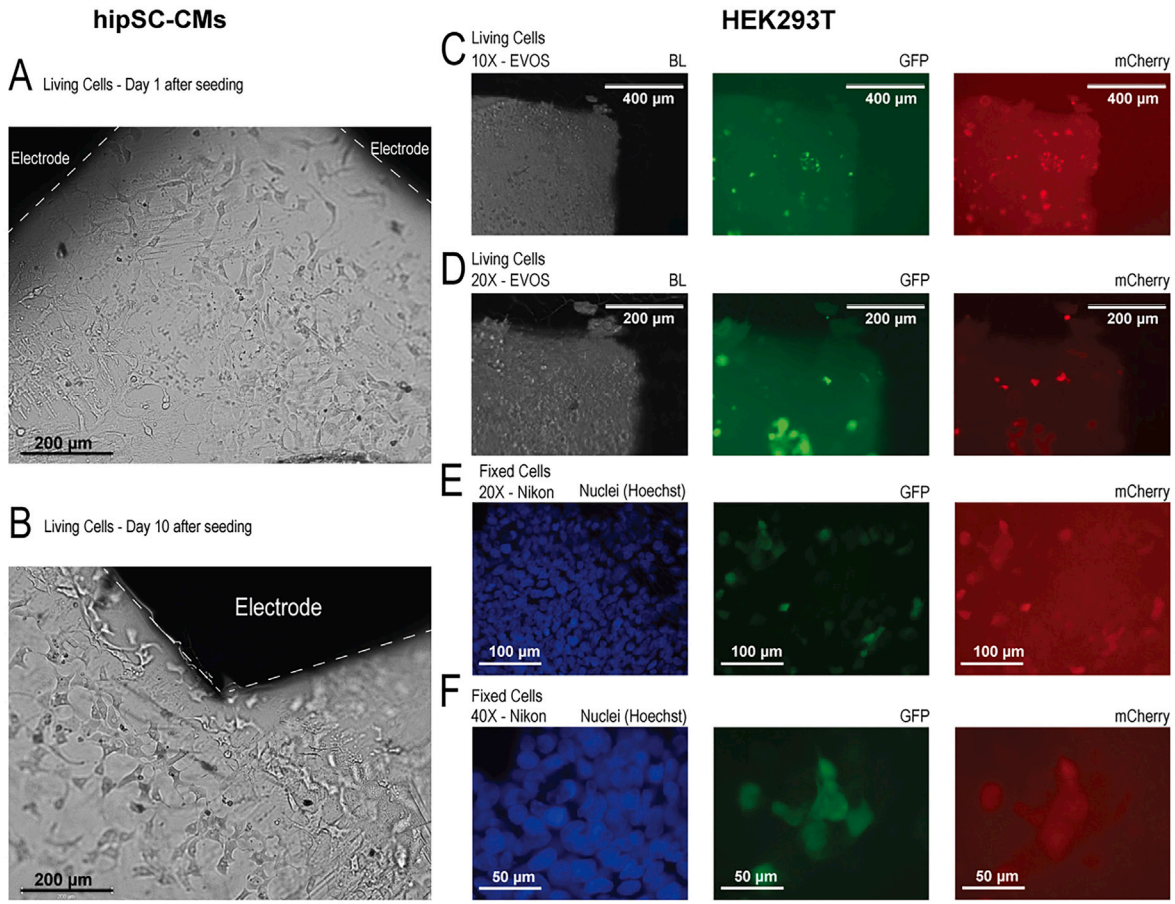


Fig. 8. (A) hiPSC-derived cardiomyocytes (hiPSC-CMs) seeded on top of the IPMC actuators and (B) maintained in culture for 10 days. Immunofluorescence imaging of HEK293T cells co-transfected with plasmids expressing GFP and mCherry fluorescent proteins. (C) Pictures at 10X and (D) 20X magnification of living HEK293T cells cultured on the transparent Nafion membrane using the EVOS™ M3000 imaging system. For both magnifications, the same area was imaged using bright light (BL) to visualize all cells, 488 nm excitation with FITC/GFP filter to visualize GFP-positive cells, and 561/587 nm excitation with TRITC/mCherry filter to visualize mCherry-positive cells, from left to right. (E) Pictures at 20X and (F) 40X magnification of HEK293T cells cultured on the transparent Nafion membrane after fixation, permeabilization, nuclei staining and coverslip mounting. Images were acquired using a Nikon Eclipse 80i. For both magnifications, the same area was imaged using (from left to right) 350–405 nm excitation with DAPI filter (Hoechst) to visualize cell nuclei, 488 nm excitation with FITC/GFP filter to visualize GFP-positive cells, and 561/587 nm excitation with TRITC/mCherry filter to visualize mCherry-positive cells. For both imaging microscopes the excitation light was provided from the bottom and image acquisition from the top.

Supplementary Data. Cells seeded at comparable initial densities exhibited similar proliferation behavior under both culture conditions and reached near-complete confluence within 3 days post seeding. These observations indicate that the actuator substrate supports cell attachment and proliferation to an extent comparable to that of conventional tissue culture substrates, further demonstrating its cytocompatibility.

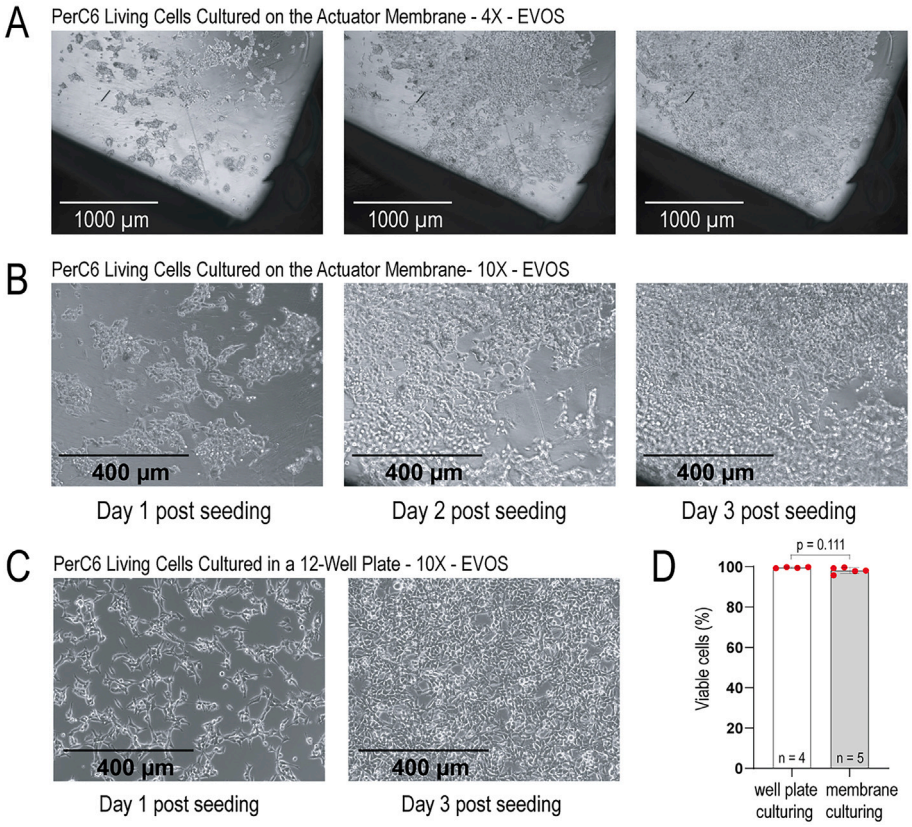


Fig. 9. (A,B) Representative bright-field optical images of PER.C6 cells cultured on the actuator at 4× and 10× magnification, respectively. (C) Representative image of PER.C6 cells cultured in a conventional 12-well plate (control condition). (D) Quantitative comparison of PER.C6 cell viability between cells cultured on the actuator and in a conventional 12-well plate. Cell viability was assessed by Trypan Blue exclusion and automated cell counting. Error bars denote the standard deviation, and statistical significance was evaluated using a Mann–Whitney *U* test ($p = 0.111$). (For Interpretation of the references to colour in this figure legend, the reader is referred to the web version of this article.)

To quantitatively evaluate cytocompatibility under the two culture conditions, cell viability was determined by Trypan Blue exclusion, whereby live cells with intact membranes remain impermeable to the dye, while dead cells are stained blue. For the 36 viability measurements performed, an average of 1,681,676 ± 573,307 cells (mean ± SD, $n = 36$) were counted per measurement. Cell viability, expressed as the percentage of live cells relative to the total number of cells, is presented in Fig. 9(D) (also Table S1). Statistical analysis using a Mann–Whitney *U* test revealed no significant difference in cell viability between cells cultured on Nafion membranes and those cultured in conventional well plates ($p = 0.111$). Together with the observed comparable proliferation, these findings indicate that the actuator provides a cytocompatible substrate capable of supporting cell attachment, growth, and survival similarly to standard tissue culture surfaces. Although classical mechanobiology studies typically apply cyclic strains in the range of 1–10% to elicit robust changes in cytoskeletal organization, focal adhesion dynamics, or gene expression, emerging evidence demonstrates that certain cellular processes are sensitive to mechanical perturbations several orders of magnitude smaller. Nuclear mechanotransduction, for example, has been shown to respond to submicrometer deformations that impose only microstrain-level changes on the cell, with even very small substrate displacements transmitting mechanical load to the nuclear lamina and influencing chromatin organization [25]. Likewise, mechanosensitive ion channels such as Piezo1 can activate under extremely small increases in membrane tension when cytoskeletal buffering is reduced, indicating that whole-cell strains well below 1% can still modulate mechanotransductive signaling [7]. Cancer cells also exhibit heightened sensitivity to minimal mechanical deformation, where compression-induced microstrains alter nuclear shape and promote invasive phenotypes despite the absence of large-scale tissue stretch [50]. Similarly, developing neurons are capable of detecting nanoscale mechanical cues that guide axon extension and pathfinding, again operating within a deformation regime far below percent-level strain [11]. Together, these findings support the notion that a soft biocompatible actuator capable of generating approximately 0.01% cyclic strain may serve as a valuable platform for probing ultra-sensitive mechanobiological responses, particularly in nuclear mechanics, ion-channel-mediated signaling, cancer mechanoadaptation, and neuronal mechanoguidance. Importantly, this strain level does not represent a fundamental limitation of the fabrication strategy itself; rather, the present implementation establishes a baseline upon which multiple strain-amplification strategies, including geometric optimization, multilayer stacking (combined with other EAPs), electrode pattern engineering, increasing the actuation voltage, and decreasing the core polymer thickness, can be systematically evaluated. Thus, while the current actuator operates in the microstrain regime, the fabrication approach remains flexible and scalable for exploring enhanced strain outputs in future iterations.

5. Conclusion

In this work, we introduced and characterized a partially-transparent IPMC actuator designed for integration into microphysiological systems to study the effects of mechanical stimulation on cell monolayers. The device employs patterned Au and Pt electrodes deposited by e-beam evaporation, enabling electrode definition while accommodating the

processing constraints of the Nafion ionomer substrate. Conventional adhesion layers were avoided because they interfere with ion transport and degrade actuation performance. Instead, a thin parylene-C encapsulation layer was employed to enhance electrode stability without compromising optical clarity. Comprehensive characterization, including electrical, mechanical, electromechanical, optical, and biological evaluations, demonstrated that the actuator can reliably generate sub-percent strain while maintaining partial optical transparency. These results highlight the potential of the proposed platform for delivering controlled mechanical stimuli to investigate mechanotransduction mechanisms in cellular systems.

CRediT authorship contribution statement

Alireza Tajeddin: Writing – review & editing, Writing – original draft, Visualization, Validation, Software, Methodology, Investigation, Formal analysis, Data curation, Conceptualization. **Antonio Velarte:** Software, Methodology, Investigation. **Romina Sattari:** Resources, Data curation. **Maury Wiendels:** Methodology, Investigation. **Andres Hunt:** Writing – review & editing, Supervision. **Christine L. Mummery:** Writing – review & editing, Writing – original draft, Supervision. **Valeria Orlova:** Writing – review & editing, Supervision, Conceptualization. **Juan Zhang:** Investigation. **Vincent Portero:** Writing – review & editing, Writing – original draft, Supervision. **Esther Pueyo:** Supervision, Funding acquisition. **Arantxa Otín:** Supervision, Resources. **Massimo Mastrangeli:** Writing – review & editing, Supervision, Resources, Project administration, Methodology, Investigation, Funding acquisition, Data curation, Conceptualization.

Declaration of competing interest

The authors declare that they have no known competing financial interests or personal relationships that could have appeared to influence the work reported in this paper.

Acknowledgements

The authors would like to thank the staff at the Else Kooi Laboratory of TU Delft for their support. This work was funded by the Netherlands Organ-on-Chip Initiative (NOCI), an NWO Gravitation project funded by the Ministry of Education, Culture and Science of the Government of the Netherlands (024.003.001). Additional support was provided by Agencia Estatal de Investigación–Ministerio de Ciencia e Innovación through projects PID2022-140556OB-I00 and TED2021-130459B-I00, by Gobierno de Aragón through the BSICoS group T39-23R and the GEPM group T23-23R, and by the UZ-Aspanoa Chair (C108/2023 3). The authors also gratefully acknowledge Brian Istvan Giam for his contributions to transparency measurements.

Appendix A. Supplementary data

Supplementary data for this article can be found online at doi:10.1016/j.sna.2026.118243.

Data availability

Data will be made available upon request.

References

[1] Y. Bar-Cohen, Electroactive Polymer (EAP) Actuators as Artificial Muscles: Reality, Potential, and Challenges, second ed, SPIE Press, Bellingham, WA, 2004.
[2] R. Barbosa, R. Goncalves, G.E. Blanco, M.C. Saccardo, R.S. Paiva, V.R. Mastelaro, S.A. Cruz, C.H. Scuracchio, Plasma treatment of nafion membranes: understanding the trade-off between surface modification and electrochemical degradation, J. Power Sources 610 (2024) 234741.
[3] B. Bhandari, G.Y. Lee, S.H. Ahn, A review on IPMC material as actuators and sensors: fabrications, characteristics and applications, Int. J. Precis. Eng. Manuf. 13 (2012) 141–163.
[4] P. Brochu, Q. Pei, Advances in dielectric elastomers for actuators and artificial muscles, Macromol. Rapid Commun. 31 (2010) 10–36, https://doi.org/10.1002/marc.200900425
[5] G. Campostrini, V. Meraviglia, E. Giacomelli, R.W. van Helden, L. Yiangou, R.P. Davis, M. Bellin, V.V. Orlova, C.L. Mummery, Generation, functional analysis and applications of isogenic three-dimensional self-aggregating cardiac microtissues from human pluripotent stem cells, Nat. Protoc. 16 (2021) 2213–2256.
[6] F. Carpi, E. Smela (Eds), Biomedical Applications of Electroactive Polymer Actuators, Wiley, Chichester, UK, 2009.
[7] C.D. Cox, N. Bae, K. Ziegler, B. Grant, S. Hall, B. Martinac, Removal of the mechanoprotective influence of the cytoskeleton reveals Piezo1 is tuned to membrane tension, Nat. Commun. 7 (2016) 10366.
[8] X. Di, X. Gao, L. Peng, J. Ai, X. Jin, S. Qi, H. Li, K. Wang, D. Luo, Cellular mechanotransduction in health and diseases: from molecular mechanism to therapeutic targets, Signal Transduct. Target. Ther. 8 (2023) 282.
[9] D.E. Discher, P. Janmey, Y.L. Wang, Tissue cells feel and respond to the stiffness of their substrate, Science 310 (2005) 1139–1143.
[10] X. Fang, P. Wang, F. Lin, J. Huang, J. Fang, C. Xiong, Pneumatic cell stretching chip to generate uniaxial strain using an elastomeric membrane with ridge structure, Chemosensors 10 (2022) 302.
[11] K. Franze, The mechanical control of nervous system development, Development 140 (2013) 3069–3077.
[12] G. Gallucci, A. Hunt, Poly (vinylidene fluoride)-based ferroelectric polymers for electromechanical transduction: a systematic review of materials and actuators, Adv. Intell. Syst. (2025) e202500694.
[13] Y. Gao, Z. Zhang, Y. Yao, J. Zhang, X. Li, K. Yang, N. Si, Z. Chen, Z. Gu, N. Yin, Engineering of tissue in microphysiological systems demonstrated by modelling skeletal muscle, Regen. Biomater. 12 (2025) rbaf059. https://academic.oup.com/rb/article/doi/10.1093/rb/rbaf059/8164132
[14] T. Gierke, G. Munn, F. Wilson, The morphology in nafion perfluorinated membrane products, as determined by wide- and small-angle x-ray studies, J. Polym. Sci. Polym. Phys. Ed. 19 (11) (1981) 1687–1704.
[15] A.M. Greiner, H. Chen, J.P. Spatz, R. Kemkemer, Cyclic tensile strain controls cell shape and directs actin stress fiber formation and focal adhesion alignment in spreading cells, PLoS One 8 (2013) e77328.
[16] M. Hao, Y. Wang, Z. Zhu, Q. He, D. Zhu, M. Luo, A compact review of IPMC as soft actuator and sensor: current trends, challenges, and potential solutions from our recent work, Front. Robot. AI 6 (2019) 129.
[17] D. Huh, B.D. Matthews, A. Mammoto, M. Montoya-Zavala, H.Y. Hsin, D.E. Ingber, Reconstituting organ-level lung functions on a chip, Science 328 (2010) 1662–1668.
[18] D.E. Ingber, Cellular mechanotransduction: putting all the pieces together again, FASEB J. 20 (2006) 811–827.
[19] J.H. Jeon, S.W. Yeom, I.K. Oh, Fabrication and actuation of ionic polymer metal composites patterned by combining electroplating with electroless plating, Compos. A Appl. Sci. Manuf. 39 (2008) 588–596.
[20] D. Joseph, et al., Porous nafion membranes, J. Membr. Sci. 520 (2016) 723–730.
[21] S. Jungbauer, H. Gao, J.P. Spatz, R. Kemkemer, Two characteristic regimes in frequency-dependent dynamic reorientation of fibroblasts on cyclically stretched substrates, Biophys. J. 95 (2008) 3470–3478.
[22] Y. Ke, et al., A critical review on surface-pattern engineering of nafion membranes for advanced fuel cells, Renew. Sustain. Energy Rev. 145 (2021) 110860.
[23] K.J. Kim, S. Tadokoro, Electroactive Polymers for Robotic Applications: Artificial Muscles and Sensors, Springer, London, 2007.
[24] K.J. Kim, S. Tadokoro, Ionic polymer–metal composite actuators: modeling and simulation, J. Intell. Mater. Syst. Struct. 18 (2007) 39–45.
[25] T.J. Kirby, J. Lammerding, Emerging views of the nucleus as a cellular mechanosensor, Nat. Cell Biol. 20 (2018) 373–381.
[26] J. Kreutzer, M. Viehrig, R.P. Pölönen, F. Zhao, M. Ojala, K. Aalto-Setälä, P. Kallio, Pneumatic unidirectional cell stretching device for mechanobiological studies of cardiomyocytes, Biomech. Model. Mechanobiol. 19 (2020) 291–303.
[27] K. Kurpinski, S. Li, Mechanical stimulation of stem cells using cyclic uniaxial strain, J. Vis. Exp. JoVE (2007) 242.
[28] A. Kusoglu, A.Z. Weber, New insights into perfluorinated sulfonic-acid ionomers, Chem. Rev. 117 (2017) 987–1104.
[29] J. Lai, B. Zeng, J. Liu, J. Zhang, W. Pei, Y. Zhou, Y. Liu, J. Li, Y. Tong, Current research status of ionic polymer–metal composites in applications of low-voltage actuators, Mater. Adv. 5 (2024) 4601–4617.
[30] J.C. Lien, Y.L. Wang, Cyclic stretching-induced epithelial cell reorientation is driven by microtubule-modulated transverse extension during the relaxation phase, Sci. Rep. 11 (2021) 14803.
[31] J. Liu, K.J. Kim, Dynamic mechanical analysis of ionic polymer–metal composites under various hydration levels, J. Appl. Polym. Sci. 137 (2020) 48673.
[32] J.D.W. Madden, Conducting polymer actuators, J. Micromech. Microeng. 10 (2000) 101–119, https://doi.org/10.1088/0960-1317/10/1/316
[33] M. Mastrangeli, J. van den Eijnden-van Raaij, Organs-on-chip: the way forward, Stem Cell Rep. 16 (2021) 2037–2043.
[34] F. Michielin, E. Serena, P. Pavan, N. Elvassore, Microfluidic-assisted cyclic mechanical stimulation affects cellular membrane integrity in a human muscular dystrophy in vitro model, RSC Adv. 5 (2015) 98429–98439.
[35] A.G. Monteduro, S. Rizzato, G. Caragnano, A. Trapani, G. Giannelli, G. Maruccio, Organs-on-chips technologies–a guide from disease models to opportunities for drug development, Biosens. Bioelectron. 231 (2023) 115271.
[36] P. Motreuil-Ragot, A. Hunt, L.N. Sacco, P.M. Sarro, M. Mastrangeli, Manufacturing thin ionic polymer metal composite for sensing at the microscale, Smart Mater. Struct. 32 (2023) 035006.
[37] P. Motreuil-Ragot, A. Hunt, D. Kasi, B. Brajon, A. van den Maagdenberg, V. Orlova, M. Mastrangeli, P.M. Sarro, Enabling actuation and sensing in organs-on-chip using electroactive polymers, in: 2020 3rd IEEE International Conference on Soft Robotics (RoboSoft), IEEE, 2020, pp. 530–535.

[38] S. Nemat-Nasser, J.Y. Li, Electromechanical response of ionic polymer–metal composites, J. Appl. Phys. 87 (2000) 3321–3331, https://doi.org/10.1063/1.372331
[39] B.W. Ninham, M.J. Battye, P.N. Bolotskova, R.Y. Gerasimov, V.A. Kozlov, N.F. Bunkin, Nafion: new and old insights into structure and function, Polymers 15 (2023) 2214.
[40] R. Pelrine, R. Kornbluh, Q. Pei, J. Joseph, Dielectric elastomer actuators for microrobotics and biomedical devices, in: Proceedings of SPIE – Smart Structures and Materials 2000: Electroactive Polymer Actuators and Devices, 2000, pp. 126–137, https://doi.org/10.1117/12.344863
[41] S.J. Pratt, C.M. Plunkett, G. Kuzu, T. Trinh, J. Barbara, P. Choconta, D. Quackenbush, T. Huynh, A. Smith, S.W. Barnes, et al., A high throughput cell stretch device for investigating mechanobiology in vitro, APL Bioeng. 8 (2024).
[42] S. Sadeghzadeh, K. Asaka, Mechanical and electroactive properties of nafion-based actuators with different electrode morphologies, Smart Mater. Struct. 27 (2018) 075012.
[43] E. Safronova, et al., Correlation between nafion morphology in various dispersions and properties of the cast membranes, Polymers 14 (2022) 5275.
[44] M. Shahinpoor, Y. Bar-Cohen, J. Simpson, J. Smith, Ionic polymer-metal composites (IPMCs) as biomimetic sensors, actuators and artificial muscles-a review, Smart Mater. Struct. 7 (1998) R15.
[45] M. Shahinpoor, K.J. Kim, Ionic polymer–metal composites: III. modeling and simulation of the electro-mechanics of IPMCs, Smart Mater. Struct. 23 (2014) 063001.
[46] B.H. Shin, Y.S. Kim, S.Y. Lee, Patterning method of IPMC actuator using a milling machining, Key Eng. Mater. 706 (2016) 68–72.
[47] V.K. Singh, T.M. Seed, How necessary are animal models for modern drug discovery? Expert Opin. Drug Discov. 16 (2021) 1391–1397.
[48] A.O. Stucki, J.D. Stucki, S.R. Hall, M. Felder, Y. Mermoud, R.A. Schmid, T. Geiser, O.T. Guenat, A lung-on-a-chip array with an integrated bio-inspired respiration mechanism, Lab Chip 15 (2015) 1302–1310.
[49] D. Sun, W. Gao, H. Hu, S. Zhou, Why 90% of clinical drug development fails and how to improve it? Acta Pharm. Sin. B 12 (2022) 3049–3062.
[50] J.M. Tse, G.A. Cheng, J.A. Tyrrell, R.J. Wilcox, D.J. Wolf, M.S. Lammerding, Mechanical compression drives cancer cells toward an invasive phenotype, Proc. Natl. Acad. Sci. 109 (2012) 911–916.
[51] G. Uzer, W.R. Thompson, B. Sen, Z. Xie, S.S. Yen, S. Miller, G. Bas, M. Styner, C.T. Rubin, S. Judex, et al., Cell mechanosensitivity to extremely low-magnitude signals is enabled by a LINCed nucleus, Stem cells 33 (2015) 2063–2076.
[52] G. Wang, Y. Sun, A. Ji, G. Yin, H. Ge, X. Liu, X. Tong, M. Yu, Review on the research progress and application of IPMC sensors: gengying wang et al, J. Bionic Eng. 21 (2024) 2687–2716.
[53] S. Zhang, G. Xu, J. Wu, X. Liu, Y. Fan, J. Chen, G. Wallace, Q. Gu, Microphysiological constructs and systems: biofabrication tactics, biomimetic evaluation approaches, and biomedical applications, Small Methods 8 (2024) 2300685.
[54] Q. Zhao, T. Cole, Y. Zhang, S.Y. Tang, Mechanical strain-enabled reconstitution of dynamic environment in organ-on-a-chip platforms: a review, Micromachines 12 (2021) 765.

Author biography



Alireza Tajeddin is currently pursuing the Ph.D. degree with a Electronics Components, Technology and Materials (ECTM) Group, Department of Microelectronics, Faculty of Electrical Engineering, Mathematics and Computer Science (EEMCS), Delft University of Technology (TU Delft), Delft, The Netherlands. His research focuses on BioMEMS, electroactive polymers, and the development of soft sensors and actuators for integration into organ-on-chip platforms.



Antonio Velarte Iranzo received the M.Sc. degree in Electronic Engineering from the University of Zaragoza, Zaragoza, Spain, in 2020. He is currently pursuing a Ph.D. degree in Biomedical Engineering with the Department of Electronic Engineering and Communications, University of Zaragoza, where he also serves as a substitute lecturer. His research focuses on the development of biomedical instrumentation, embedded electronic systems, and sensing technologies for cardiac and neuroscience applications.



Romina Sattari received the B.Sc. and M.Sc. degrees in Electrical Engineering from Sharif University of Technology, Tehran, Iran, in 2015 and 2017, respectively, and the Ph.D. degree from Delft University of Technology, the Netherlands, in 2025. Her Ph.D. research focused on multidomain reliability monitoring of semiconductor packages and modules. She is currently an IC Design Support Specialist with the Department of Microelectronics, TU Delft, where she contributes to various research and development projects.



Maury Wiendels received the M.S. degree in Medical Biology from Radboud University, Nijmegen, The Netherlands in 2020. She is currently pursuing the Ph.D. degree in in-vitro stem cell models at Leiden University Medical Center. Her research interests include single cell cardiomyocyte analysis with the use of UV micropatterning.



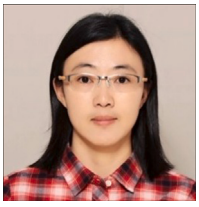
Andres Hunt is an assistant professor in the Department of Precision and Microsystems Engineering at Delft University of Technology. His research focuses on high-performance functional materials, actuators, and additive manufacturing methods to enable embedding actuation, sensing, and other intelligent functionalities into engineering materials, structures, and devices.



Christine Mummery is Professor of Developmental Biology at Leiden University Medical Center, Leiden, the Netherlands. Her research is focused on modeling cardiovascular diseases using pluripotent stem cells from patients and developing organ-on-chip models to predict toxic effects of drugs on the human heart and identify individual drug sensitivity. She was president of the International Society for Stem Cell Research (2020-2021) and co-founded the European Organ-on-Chip Society. She is a member of the Royal Netherlands Academy of Sciences and several other learned societies, and serves on various public and private advisory boards.



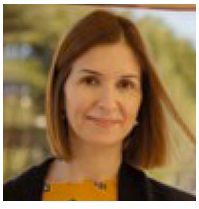
Valeria Orlova received her M.Sc. degree in Biotechnology from the Moscow State Academy of Fine Chemical Technology, Russia, in 2003, and her Ph.D. degree in Medicine from Ruprecht-Karls-University Heidelberg, Germany, in 2007. Following postdoctoral training at the Experimental Immunology Branch of the National Cancer Institute, NIH, USA, and at Leiden University Medical Center (LUMC), she is now an Associate Professor in the Department of Anatomy and Embryology at LUMC and an Associate Investigator at the Novo Nordisk Foundation Center for Stem Cell Medicine, reNEW, in the Netherlands. Her research focuses on human induced pluripotent stem cell technology, vascular biology, and vascularized 3D organ-on-chip models of cardiovascular disease.



Juan Zhang received her Ph.D. degree from Tsinghua University, Beijing, China. She currently works at the Laboratory of Experimental Cardiology, Leiden University Medical Center, Leiden, the Netherlands. Her research primarily focuses on the immortalization of human and rat cardiomyocytes.



Vincent Portero received the Ph.D. degree from the University of Nantes, Nantes, France, in 2013. He is currently an Assistant Professor at the Laboratory of Experimental Cardiology, Leiden University Medical Center, Leiden, the Netherlands. His research interests include the molecular mechanisms underlying cardiac arrhythmias and novel therapeutic strategies for atrial fibrillation.



Esther Pueyo received her Ph.D. degree in Biomedical Engineering from the University of Zaragoza, Spain, in 2006. She completed predoctoral and postdoctoral training and held visiting research positions at the University of London and the University of Oxford, UK. She is currently a Full Professor at the University of Zaragoza and a Senior Researcher at the Aragón Health Research Institute and the Center for Biomedical Network Research. Her research focuses on biomedical signal processing and multiscale computational modeling and simulation.



Aránzazu Otín is an Associate Professor in Electronic Technology at the Department of Electronic Engineering and Communications, University of Zaragoza, Spain. She received her Ph.D. degree in Electronic Engineering from the University of Zaragoza in 2007. She completed predoctoral and postdoctoral research training and held visiting research appointments at Delft University of Technology, The Netherlands. She is a member of the Power Electronics and Microelectronics Group (GEPM) within the Aragón Institute for Engineering Research (I3A). Her research interests include analog and mixed-signal integrated circuit design, bioelectronics, biosensing interfaces, and low-power electronic systems for biosignal acquisition, stimulation, and real-time monitoring.



Massimo Mastrangeli received his Ph.D. degree in materials engineering from the University of Leuven, Belgium, in 2010. He is currently an Associate Professor in the Department at Microelectronics of Delft University of Technology, the Netherlands, where he leads the MEMPhyS group in the design and fabrication of microelectromechanical physiological systems. He chairs the ISO/TC 276/SC 2 on microphysiological systems and organs-on-chip and is a member of the board of the European Organ-on-Chip Society.